A Method for Evaluating Limiting Drawing Ratios

H. Iseki and R. Sowerby

Sufficient data have now been generated to assess the influence of material, process, and tooling variables on the limiting drawing ratio, when deep drawing cylindrical cups from circular blanks. The influence of these parameters is less well understood in the deep drawing of nonaxisymmetric cups, and the data that exist have generally been collected from drawing tests. A theoretical approach is presented for predicting the limiting drawing ratio when deep drawing prismatic cups. For a given blank geometry, the drawing load is calculated to plastically deform the flange, overcome friction between the flange and the blank holder, and to bend the material over the die radius. Deformation in the cup wall is ignored. The onset of yielding in the flange is determined using a finite-element code. The calculated drawing load is compared to a theoretical maximum, and when the two values coincide, this yields the limiting blank size under the assumed processing conditions, i.e., blank holder force, die radius, blank shape, and coefficient of friction. The theoretical predictions were compared with experimental results when deep drawing square cups from optimum blank shapes, and the correspondence was found to be acceptable.

Keywords:
deep drawing, limiting drawing ratios, friction, ideal blank shapes, die geometry, finite elements

1. Introduction

SUFFICIENT experimental and analytical data have been assembled to make a reasonably accurate assessment of the limiting drawing ratio when producing cylindrical cups from circular blanks. The same cannot be said about the production of prismatic cups of noncircular cross section. Some data can be found in handbooks and technical papers, wherein the information generally has been produced by experimentation rather than analysis.

A number of papers have appeared on methods to predict optimum blank shapes for the production of prismatic cups.[1-7] The blanks are deemed optimum in the sense that flat-topped cups are produced, and at best, trimming of waste material can be eliminated. However, no attempt has been made to ascertain the limiting size of the optimum shaped blank.

In this article, a simplified analysis is presented for predicting the limiting size of blanks based on the attainment of a maximum drawing load. Only the onset of the drawing operation is considered and not the entire process. The drawing force is calculated to produce plasticity throughout the flange of the blank to overcome the frictional constraint and the work done in bending the material over the die radius. The analysis applies to any shape of cup and blank.

In an earlier study,[8] experiments were performed drawing square cups from optimum shaped blanks, and limiting drawing ratios were determined for a range of blank holder forces. Wrinkling limited the blank size at the lower clamping loads, whereas fracture or tearing was the failure mode at the higher blank holder loads. The present method of predicting the critical blank size agreed quite well with the experimentally determined values when failure occurred by tearing.

H. Iseki, Faculty of Engineering, Tokyo Institute of Technology, Tokyo, Japan; and **R. Sowerby,** Faculty of Engineering, McMaster University, Hamilton, Ontario, Canada.

The calculations to determine the stress and velocity distribution within the flange were based on a finite-element code developed by Iseki and Murota.[7,9]

2. Theory

2.1 *Deep Drawing of a Cylindrical Cup from a Circular Disk*

As an illustration of the technique, consider the deformation in a flange when drawing a cylindrical cup from a circular disk. The initial inner and outer radii of the flange (annulus) are r_i and r_o. If the deformation in the flange is one of plane stress, then the radial equilibrium equation is

$$\frac{d\sigma_r}{dr} + \frac{\left(\sigma_r - \sigma_\theta\right)}{r} = 0 \qquad \text{[Eq 1]}$$

Assuming the material obeys the von Mises yield criterion, the yield function in the flange can be expressed as:

$$\sigma_r^2 - \sigma_r\sigma_\theta + \sigma_\theta^2 = Y^2 \qquad \text{[Eq 2]}$$

where σ_r, σ_θ, and Y denote the radial, hoop, and yield stress, respectively. Eliminating σ_θ from Eq 1 and 2 yields:

$$\frac{dr}{r} = \frac{-2d\sigma_r}{\left[\left(4Y^2 - 3\sigma_r^2\right)^{1/2} + \sigma_r\right]} \qquad \text{[Eq 3]}$$

The solution of the above differential equation with the boundary condition

$$\sigma_r = 0 \text{ at } r = r_o \qquad \text{[Eq 4]}$$

is

$$\ln\left(\frac{r}{r_o}\right) = -\left\{\frac{\sqrt{3}}{2}\sin^{-1}B + \frac{1}{2}\ln\left(\left[1 - B^2\right]^{1/2} + \frac{B}{\sqrt{3}}\right)\right\} \qquad \text{[Eq 5]}$$

where

$$B = \frac{\sqrt{3}\,\sigma_r}{2Y}$$

If the initial thickness of the material is t, the drawing force, P, at the inside radius r_i can be expressed as:

$$P = 2\pi r_i \sigma_r t \qquad \text{[Eq 6]}$$

From Eq 2, the maximum value for σ_r is $2Y/\sqrt{3}$, and it is assumed that this represents the limiting value for stress at $r = r_i$. Therefore, within the flange, the ratio σ_r/Y varies over the range:

$$0 \le \frac{\sigma_r}{Y} \le \frac{2}{\sqrt{3}}$$

whereas from Eq 5, the corresponding range of the drawing ratio r_o/r_i is

$$1 \le \frac{r_o}{r_i} \le \frac{1}{3^{1/4}} \exp\left(\frac{\sqrt{3}}{4} \cdot \pi\right)$$

Figure 1 shows the variation in the normalized drawing force, P/P_{max}, with the drawing ratio $\beta = r_o/r_i$. The maximum drawing force P_{max} is given by Eq 6, with $\sigma_r = 2Y/\sqrt{3}$, and the maximum or limiting value of the drawing ratio is

$$\beta_{max} = \frac{1}{3^{1/4}} \exp\left(\frac{\sqrt{3}}{4} \cdot \pi\right) = 2.96 \qquad \text{[Eq 7]}$$

The limiting drawing ratio given by Eq 7 generally overestimates what is observed in practice. The theoretical value can be reduced if friction effects and redundant work in bending are taken into account. These factors are considered below. The following section presents the results of a finite-element analysis for the deformation in the flange, as a means of comparison with the simplified criterion for the limiting drawing ratio presented above.

2.2 *Finite-Element Analysis of the Deformation Within the Flange*

The material was assumed to be rigid, perfectly plastic, and because of symmetry, only a quarter of the flange was considered. The flange was discretized into 96 quadrilateral elements, eight in the radial direction and twelve in the hoop direction. Each quadrilateral element was then further subdivided across the diagonals to produce four triangles (see the inset diagram in Fig. 1). The finite-element mesh was then comprised of 384 triangular elements and 213 nodal points. The details of the finite-element method used in this study have been described elsewhere[7,9] and will not be repeated here.

Figure 1 shows the results of the calculations. For different values of r_o/r_i, the drawing force was evaluated to produce plastic deformation throughout the annulus. The numerical results agreed quite well with the analytical solution, but it was observed that the way the annulus was discretized could influence the results. If the radial direction was divided into eight equally spaced elements, the drawing force continued to increase beyond the theoretical maximum as r_o/r_i increased; this is illustrated by the square symbols in Fig. 1. The numerical results did not imply any instability in the process such as excessive thinning at the inside radius, the attainment of a load maximum, etc. To investigate the effect of discretization of the finite-element mesh on the numerical results, the following parameter was introduced:

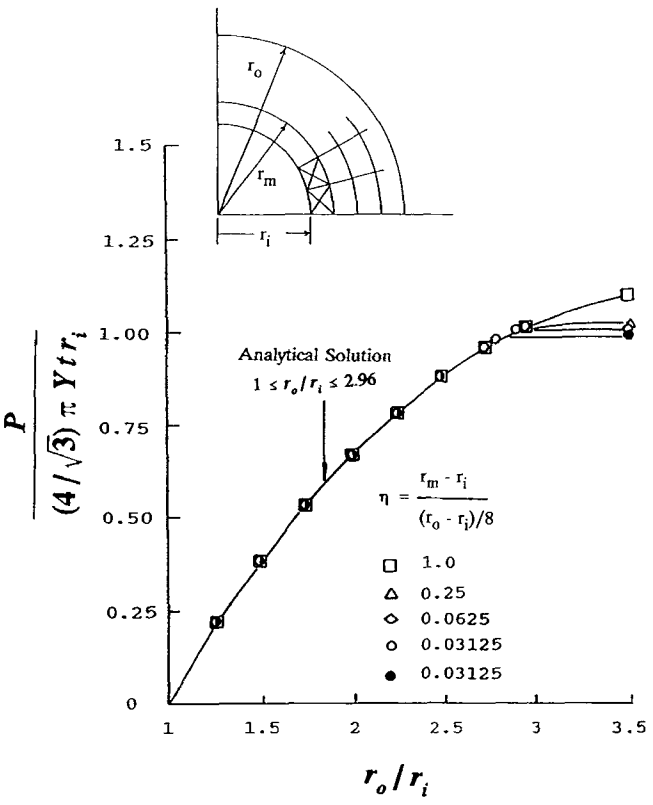

Fig. 1 Effect of finite-element mesh on calculated drawing force when deep drawing cylindrical cups.

$$\eta = \frac{\left(r_m - r_i\right)}{\left[\frac{r_o - r_i}{8}\right]} \qquad \text{[Eq 8]}$$

where r_m represents the radial position of the first element (see Fig. 1). Once the radial position of the first element has been determined by Eq 8, the remaining seven elements are equispaced across the radius of the annulus. As shown in Fig. 1, four different values for η were selected. Below a certain value for η, the calculated drawing force reached a stationary value, even though the ratio r_o/r_i continued to increase. The attainment of the stationary value was taken to signify the limiting drawing ratio. The calculations also demonstrated that considerable thinning of the elements occurred once the load reached a maximum. The results for $\eta = 0.0625$ and 0.03125 were indistinguishable; the limiting drawing ratio was calculated as 2.91, a difference of 1.7% from the analytical solution.

Some preliminary calculations were also performed to ascertain the influence of the mesh size, i.e., the number of elements. Reducing the number of elements from 8 to 4 in the radial direction and adjusting the definition of η accordingly produced the results shown by the closed circles in Fig. 1, with $\eta = 0.03125$. In this case, the maximum load and limiting

drawing ratio were reduced vis à vis the analytical solution. The error was 5.4% in the limiting drawing ratio, i.e., 2.8 as opposed to 2.96.

Figure 1 shows that, at the lower values of r_o/r_i, the variation in the drawing force is almost linear. The agreement between the finite-element results and the theoretical solution is particularly good in this region. It will also be noted in Fig. 1 that the pattern of the finite-element mesh, as controlled by the η-parameter, had no influence on the numerical results, at least over the range investigated. The present calculations showed that the gradient of the hoop and radial stress is small and very nearly linear at the lower values of r_o/r_i. This is the reason that η has little effect on the numerical calculations. Furthermore, halving the number of elements in the mesh had no discernible influence on the results.

Similar calculations were performed for drawing a square cup of side $2a_i$, from a square blank of side $2a_o$. Again, the finite-element calculations were performed for the flange region only up to the point where all elements in the flange were deforming plastically. Material at the inside edge of the flange is assumed to be moving in at constant velocity, everywhere normal to the inside edge. The theoretical maximum for the punch load is again based on the assumption that the drawing stress attains a maximum value of $2Y/\sqrt{3}$ at the inside edge of the flange. In a similar manner to Eq 6, the maximum drawing force is

$$P_{\max} = \frac{16}{\sqrt{3}} a_i t Y \qquad \text{[Eq 9]}$$

The numerical calculations were performed in the same manner as for the annulus. The same number of elements and nodes were used along with the discretization parameter, η, defined as:

$$\eta = \frac{\left(a_m - a_i\right)}{\left[\frac{a_o - a_i}{8}\right]} \qquad \text{[Eq 10]}$$

The details are shown in the inset diagram in Fig. 2. The results are shown in Fig. 2, with the notation the same as that used in Fig. 1. With $\eta = 0.0625$ and 0.03125, the calculated load attains a stationary value when the ratio a_o/a_i reaches 3.5. The maximum load is close to the "theoretical" maximum, as shown in Fig. 2. Reducing the mesh size can still result in a stationary value for the drawing load; these results are shown by the closed circles in Fig. 2. In this case, the limiting drawing ratio (a_o/a_i) is about 3.1.

As shown in Fig. 2, the increase in the calculated drawing force is essentially linear at low values of a_o/a_i, and the η-parameter had little influence on the numerical results, at least over the range investigated. However, reducing the number of elements in the finite-element mesh was found to have an effect. As shown in Fig. 2, the calculated values of drawing load were increased at low values of a_o/a_i.

In the next two sections, the influence of friction and work done to bending are considered.

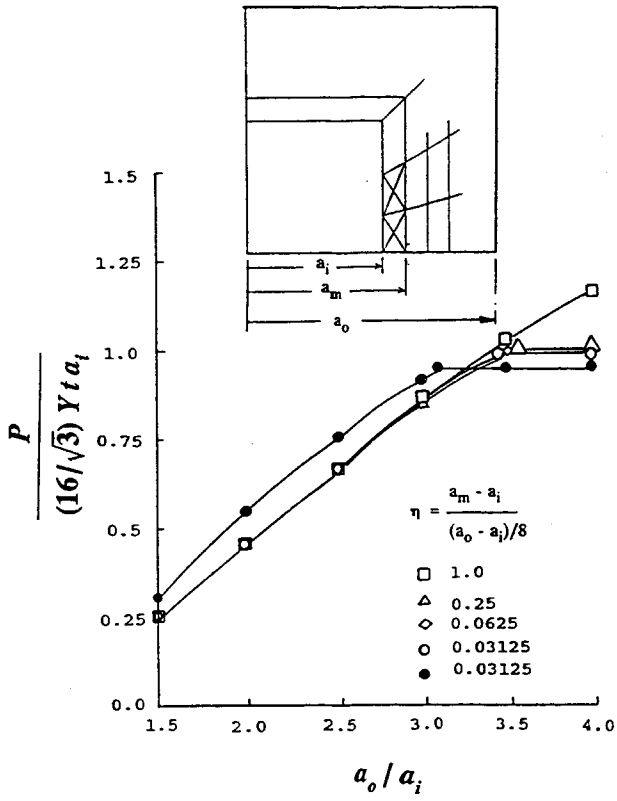

Fig. 2 Effect of finite-element mesh on calculated drawing force when deep drawing square cups from square blanks.

2.3 *Influence of Friction on the Drawing Ratio*

It is assumed that Coulomb friction acts over the top and bottom surface of the flange. In practice, the cup will be drawn in the presence of a blank holder; thus friction will be present on the upper surface of the flange. The presence of a blank holder does not negate the assumption of plane stress in the finite-element calculations of the preceding section. The normal stresses created by the blank holder are usually quite small compared to the yield stress, Y, of the material. In this work, a factor of 0.01 is used. For simplicity, it is assumed that the blank holder is in contact with the entire surface of the flange, and thus, the blank holder force, H_b, is calculated from:

$$H_b = 0.01\, Y A_f \qquad \text{[Eq 11]}$$

where A_f is the area of the flange for a limiting size blank, i.e., a blank that corresponds to the limiting drawing ratio calculated in the preceding section. The components of the nodal frictional force (R_x, R_y) are assumed to act in the plane of the flange and are calculated from:

$$\begin{Bmatrix} R_x \\ R_y \end{Bmatrix} = \frac{-2\mu H_w}{\left(V_x^2 + V_y^2\right)^{1/2}} \begin{Bmatrix} V_x \\ V_y \end{Bmatrix} \qquad \text{[Eq 12]}$$

where V_x and V_y are the velocity components, and H_w is the blank holder force at each nodal point calculated in the finite-element program.

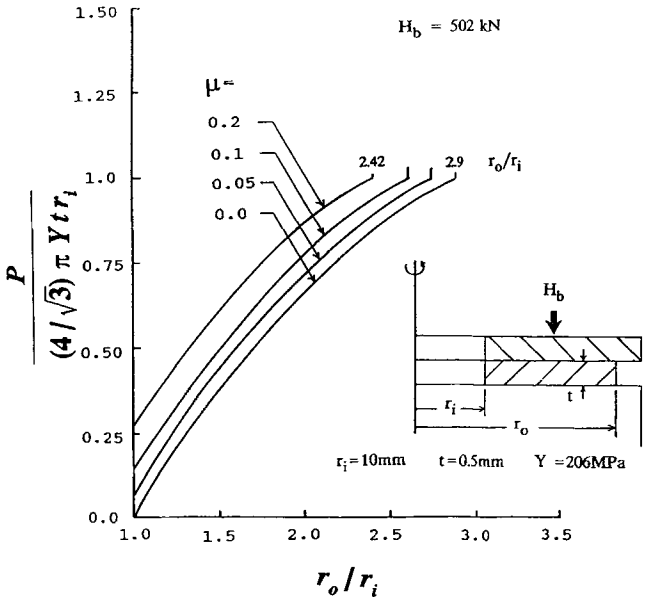

Fig. 3 Effect of the coefficient of friction on the drawing force when drawing cylindrical cups from circular blanks.

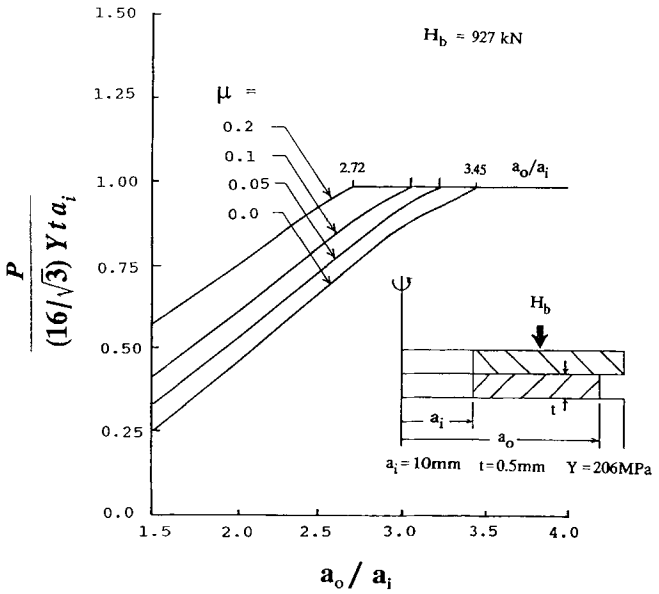

Fig. 4 Effect of the coefficient of friction on the drawing force when deep drawing square cups from square blanks.

The effect of varying the coefficient of friction for the circular blank is shown in Fig. 3. The calculations were performed for a blank with r_i = 10 mm and t = 0.5 mm. The yield stress of the material was 206 MPa and the blank holder force was 5.02 kN. Due to the presence of friction, the stationary drawing force is calculated to occur at a lower limiting drawing ratio. The bigger the coefficient of friction, the lower the limiting drawing ratio.

Similar results were found for the square blank shown in Fig. 4. Here, the hold down force was set at 9.27 kN and a_i = 10 mm.

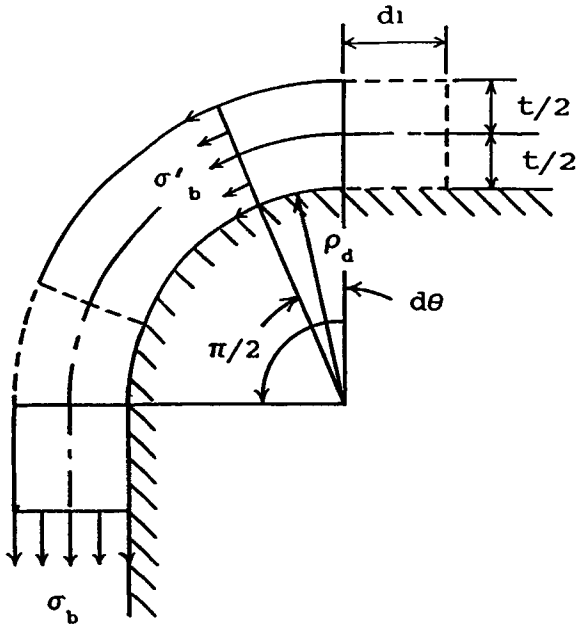

Fig. 5 Drawing a strip over the die radius.

2.4 *Effect of Bending at the Die Radius*

Study of the bending and unbending as the material passes over the die radius has been conducted by many investigators. In this work, a simple model due to Siebel[10] is adopted. The details are shown in Fig. 5, where a strip of unit width is bent over a die of radius ρ. The work done on an element of material (per unit width) as it is bent through an angle $d\theta$ is $Md\theta$, where M is the plastic bending moment $Yt^2/4$. The bending work is assumed to be equal to that done by a uniform tensile stress, σ_b, that causes the elongation $(\rho + t/2)d\theta$. Hence:

$$\sigma_b \cdot t\left(\rho + \frac{t}{2}\right)d\theta = Md\theta = Y\frac{t^2}{4}d\theta \qquad \text{[Eq 13]}$$

and

$$\sigma_b = \frac{t \cdot Y}{\left[4\left(\rho + \frac{t}{2}\right)\right]} \qquad \text{[Eq 14]}$$

If friction, μ, is assumed to act over the die nose radius, then the tensile stress is increased as the material passes over the die radius to maintain equilibrium. A simple "belt-friction" model is assumed, and hence, there is an additional term to be added to Eq 14 to obtain the stress at θ = π/2. The final result is

$$\left(\sigma_b\right)_{\theta=\frac{\pi}{2}} = \frac{\left[1 + \exp\left(\frac{\pi\mu}{2}\right)\right] t \cdot Y}{\left[4\left(\rho + \frac{t}{2}\right)\right]} \qquad \text{[Eq 15]}$$

If the circumferential length of the inner boundary is L, then the additional force, F, to be added to the nodes at the inside edge of the flange to overcome the bending and frictional effects over the die radius is

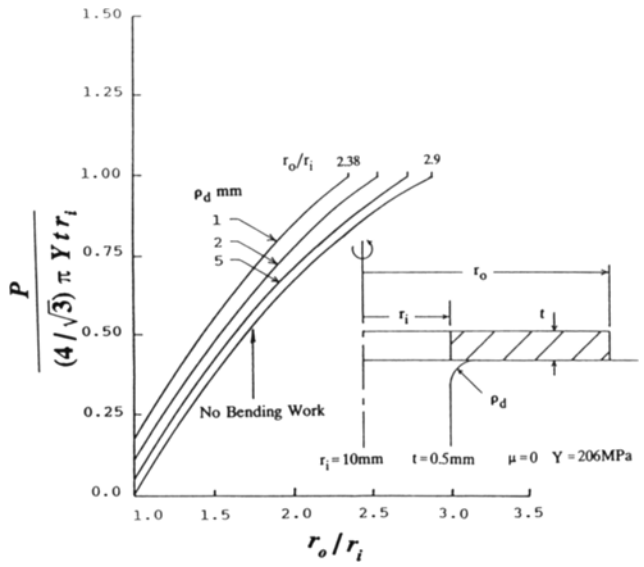

Fig. 6 Effect of die radius on drawing force when deep drawing cylindrical cups from circular blanks.

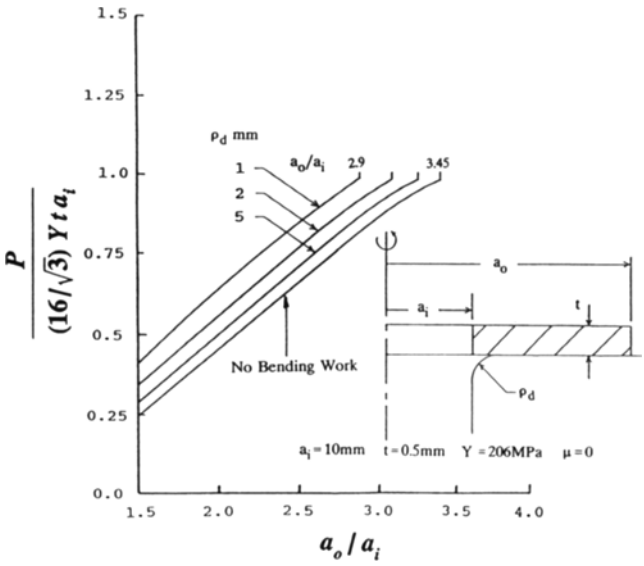

Fig. 7 Effect of die radius on drawing force when deep drawing square cups from square blanks.

$$F = \frac{\left[1 + \exp\left(\frac{\pi\mu}{2}\right)\right] t^2 L Y}{\left[4\left(\rho + \frac{t}{2}\right)\right]} \qquad \text{[Eq 16]}$$

Figure 6 shows the influence of the die radius, ρ, on the drawing force. The calculations were performed for the circular disk, inside radius r_i = 10 mm, with μ = 0. As the die radius, ρ, is reduced, the stationary drawing force is achieved at a lower value of limiting drawing ratio. Figure 7 shows similar results for the square flange.

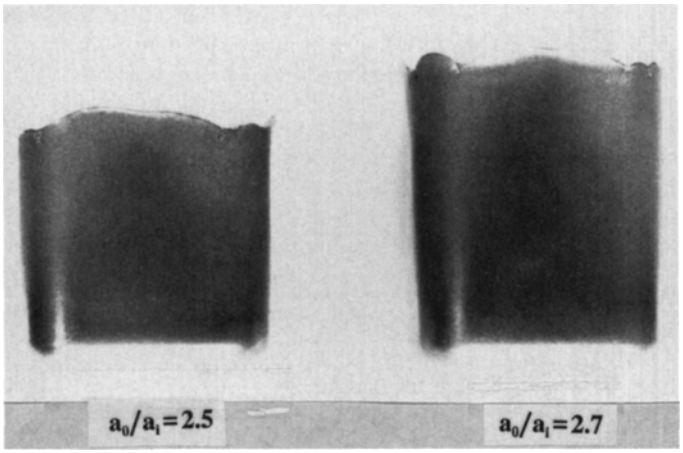

Fig. 8 Square cups drawn from optimum shaped blanks.

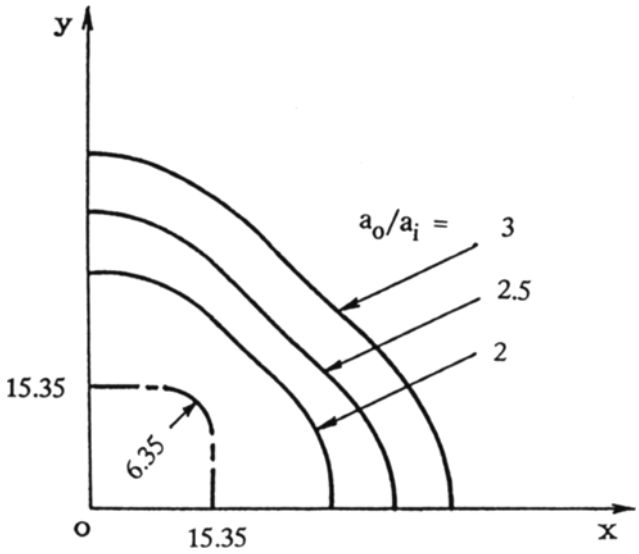

Fig. 9 Optimum blank profiles for a square punch.

3. Comparison of the Model with Experimental Data

3.1 *Experimental Data*

In a previous article, Iseki and Murota[7] used a finite-element code to predict optimum blank shapes when deep drawing square cups. The blanks were designed to produce flat-topped cups and thus eliminate the need to trim unwanted material from the drawn product. As is well known, square cups drawn from square blanks possess very large "wolf's-ears," which must be cropped from the rim of the cup. This makes square blanks impracticable for a fully drawn product.

Experiments were performed in Ref 8 to demonstrate that the optimum blank shapes did produce cups with very little undulation around the rim. Some typical drawn cups are shown in

Fig. 8. The experiments were performed on 0.5-mm thick brass sheet; the material was essentially planar isotropic, and the uniaxial stress-strain curve was fitted by the following empirical equation:

$$\sigma = 130(1 + 22\varepsilon)^{0.6} \text{ MPa}$$

Some of the optimum blank profiles calculated in Ref 8 are shown in Fig 9; also indicated are the cross-sectional dimensions of the square punch. The punch nose radius was 3 mm, as was the die radius, i.e, $\rho = 3$ mm. As illustrated in Fig. 9, the drawing ratio was defined as a_o/a_i, and the objective was to predict the limiting drawing ratio using the technique presented in the preceding sections.

Experiments were performed to determine the limiting blank size. One variable in the experimental arrangement was the blank holding force, and this could be adjusted up to a maximum of 34.9 kN (7840 lb). An attempt was made to keep the frictional conditions constant for each drawing test. Teflon sheet coated with molybdenum disulfide was used as the lubricating medium. The results are shown in Fig. 10; the closed circles represent failure by tearing or rupture, whereas the triangles indicate failure by wrinkling in the flange. Wrinkling occurs as the blank holder force is reduced, and this failure mode had not been considered in the numerical model. Consequently, predictions for the limiting drawing ratio were restricted to blank holder loads between 17.5 and 39.8 kN.

The calculations were performed assuming a coefficient of friction of $\mu = 0.05$, and the results are shown by the line in Fig. 10. Agreement with the experimental data is not unreasonable, particularly if the regime where wrinkling occurred is ignored.

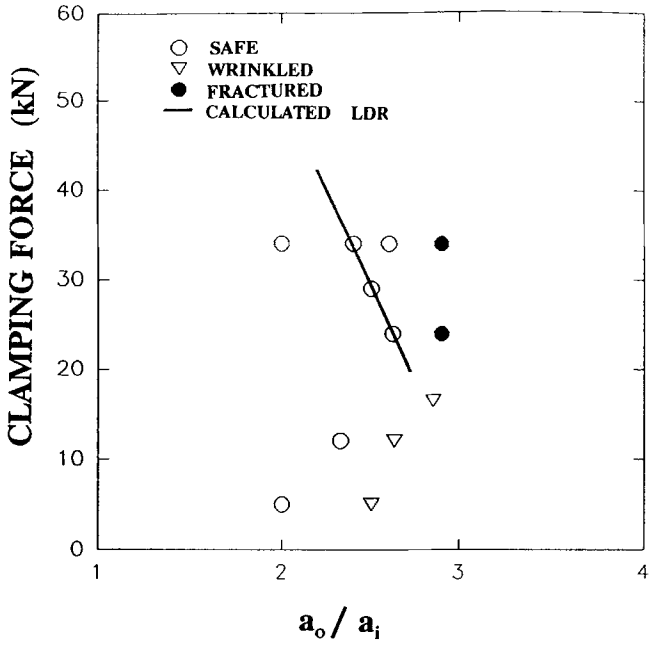

Fig. 10 Comparison of experimental and calculated limiting drawing ratios as a function of clamping force during the production of square cups from optimum blanks.

4. Conclusions

The proposed numerical procedure for calculating limiting drawing ratios when deep drawing prismatic cups has provided reasonable agreement with experimentally determined limiting drawing ratios when deep drawing square cups from ideal (or optimum) shaped blanks. The variable in the experiments was the blank holder force.

The complete drawing operation was not modeled. However, the numerical technique allowed systematic investigation of the influence of processing parameters like punch and blank shape, coefficient of friction, blank holder force, die radius, etc., on the limiting drawing ratio. The computational effort to generate the limiting drawing ratio was minimal.

Acknowledgments

The authors would like to thank the Natural Sciences and Engineering Research Council of Canada and the Manufacturing Research Corporation of Ontario for financial support.

References

1. T. Jimma, Deep Drawing of Convex Polygon-Shells, *J. Jpn. Soc. Technol. Plast.*, Vol 11, 1970, p 653-660 (in Japanese)
2. V.V. Hazek and K. Lange, Use of the Slip Line Field Method in Deep Drawing Large Irregular Shaped Components, *Proc. 7th NAMRC*, SME, 1979, p 65-71
3. H. Gloeckl and K. Lange, Computer Aided Design of Blanks for Deep Drawn Irregular Shaped Components, *Proc. 11th NAMRC*, SME, 1983, p 243-251
4. R. Sowerby, N. Chandrasekaren, X. Chen, M. Rooks, and P. Correa, The Development of Computer Aids for Sheet Metal Stampings, in *CAD/CAM and FEM in Metalworking*, S.K. Ghosh and A. Niku-Lari, Ed., Pergamon Press, 1988, p 187-203
5. C.H. Toh and S. Kobayashi, Deformation Analysis and Blank Design in Square Cup Drawing, *Int. J. Machine Tool Design Res.*, Vol 25, 1985, p 15-32
6. F. Liu, R. Sowerby, P.C. Chakvavarti, and X. Chen, The Development of Near Net Shaped Blanks for Deep Drawing Operations, *Proc. 28th Matador Conf.*, MacMillan Education Ltd., 1990, p 347-357
7. H. Iseki and T. Murota, On the Determination of the Optimum Blank Shape of Non-Axisymmetric Drawn Cups by the Finite Element Method, *Bull. ISME*, Vol 29, 1986, p 1033-1040
8. H. Iseki and T. Murota, On the Maximum Drawing Height of Square Cups from Optimum Shaped Blanks During Deep Drawing, *Proc. 33rd Jpn. Joint Conf. Tech. Plast.*, 1982, p 59-62
9. H. Iseki and T. Murota, Analysis of Deep Drawing of Non-Axisymmetric Cups by the Finite Element Method, *Proc. 1st ICTP*, Tokyo, 1984, p 678-684
10. E. Siebel and H. Beisswanger, *Tiefziehen*, Carl Hansen Verlag, Munich, 1955